TURBULENT TRAILING VORTEX WITH CENTRAL JET OR WAKE

by
J.A.H. GRAHAM, B.G. NEWMAN and W.R. PHILLIPS

4 pages missing

Pages 278 and 279 were not printed in the proceedings

Also pages 282 and 283 were not printed

from laboratory studies to full scale flight even though both flows are fully turbulent and away from solid boundaries. Full scale vortices decay more slowly than laboratory experiments would predict. In fact $\alpha = \frac{\nu_T}{\Gamma_\infty}$ decreases by a factor of 10 when the Reynolds number changes from 2×10^3 to 10^7. Owen[11] (1970) attempted to explain this with a relatively complex model of a turbulent vortex having a two-dimensional mean field and the three annular regions, an inner forced vortex region, a middle region of constant angular velocity, and an outer irrotational region. Turbulence is produced in the middle region where there is both a rate of strain and a background level of turbulence: the turbulence is then diffused into the core of solid body rotation. Owen retains the viscous terms in the equation describing conservation of mean angular momentum and this makes the final solution viscous dependent. Specifically the maximum circumferential velocity is given by

$$V_1 = \frac{\Lambda^{-1}}{4\pi} (\Gamma_\infty/\nu)^{3/4} (\nu/t)^{1/2}$$

Squire's constant α is given by $\Lambda^2 (\Gamma_\infty/\nu)^{-1/2}$, where Λ is found to be nearly the same in laboratory and flight experiments and to have a value of about 1.

Saffman[12] (1973) has also tried to explain the Reynolds number dependence by postulating a triple-structured vortex. He shows that for a two-dimensional, self-similar inviscid vortex, both the circulation and the shearing stress must approach zero like r^2 at the centre of the vortex. This generates an integral condition on the distribution of shear stress. He finds this condition implausible and suggests that the circulation at the centre is brought to zero by viscous action thus making the overall growth of the vortex dependent on Reynolds number.

When this project was started the situation was that a great deal of theoretical work had been done, without many accompanying experiments to cast light on the status of the many assumptions and predictions. In addition, the advent of large aircraft and the era of airport congestion, made the control of trailing vortices an attractive proposition.

Poppleton[13] (1971) set up a computer controlled experiment to gather data on a number of vortex flows at McGill. Our aim was to enlarge these experiments, while improving their accuracy, with an eye to finding ways of enhancing single vortex decay.

As our results showed that some flows possessed an almost scalar eddy viscosity a theory based on this was developed. It is used to predict the effect that axial momentum flux has on the time taken for the maximum rotational velocity to fall to some set desired level. The results are compared with our experiments and with some full scale data.

2. Experimental Procedure

2.1 Apparatus (Fig. 1)

2.11 Wind Tunnel

The experiments were performed in the McGill Aerodynamics Laboratory 0.76 metre, open-return, circular blower tunnel, described by Vogel[14] and used by Poppleton. The working section consisted of seven individual sections each 0.915 metres long, split and hinged for easy access. Each had a wall porosity distribution arranged to give a constant static pressure along the axis when the tunnel was empty. The final distribution differed from that used by Poppleton and resulted in a more uniform pressure. The variations in pressure over a downstream distance of 5 metres was about ±0.3% of the dynamic pressure when the vortex and jet were absent and ±0.4% in the presence of the vortex alone.

2.12 Vortex Generator

The vortex generator consisted of the split wing mounted across the horizontal diameter of the throat of the wind tunnel contraction, which was designed and used by Poppleton (1971)[13]. It was supported partially by the jet pipe (7.2 mm I.D.) whose outlet was at the exit from the contraction. The wings could be set at equal and opposite angles of incidence of 0°, 3°, 6°, 9° and 12°, one half of the span inducing positive lift and the other half negative. Each wing was designed to concentrate the trailing vortex in a narrow region about the tunnel axis, having a constant circulation with a sinusoidal transition in the centre extending over a diameter of 50.8 mm.

The traverse gear moved on a horizontal streamlined bar set between the two halves of a working section module. It allowed the probe horizontal and vertical movement over a large area of the tunnel cross section. The probe holding arrangement was improved after preliminary work. The holder was extended 200 mm further forward of the traverse gear than the arrangement used by Poppleton. This reduced the interference effects at the probe so that the pressure increase there was less than 1% of the dynamic pressure. The gear was also made lighter and more rigid. Azimuthal rotation was provided and remotely driven by cable.

2.2 Flow Arrangements

The experimental flows consisted of vortices shed by the generator in streaming flow at an angle of incidence of ±9°, interacting with a variety of jets and wakes. Mean tunnel speed was 21.4 metres/sec. in all cases.

The momentum flux increment or decrement, J is used as a measure of strength of the jets and wakes. It is given by the profile of mean axial velocity,

$$J = 2\pi\rho \int_0^\infty U\,(U-U_\infty)\,r\,dr$$

The simplest flow to arrange was that of the vortex with the coaxial wake resulting from the nacelle on the jet delivery pipe and the wrapping up of the wakes from the vortex generator. This is called 'the weak wake'. The following axial flow conditions were used:

A. a 'strong' jet, created by a 17.3 psi (1.194×10^2 kN/m^2) supply pressure, and known from preliminary measurements to cause substantial diminution of maximum rotational velocities in the vortex within the working section of the wind tunnel. Velocity increment at the first station was 26.4%, of the free stream velocity, while $\frac{|J|}{\rho\Gamma_\infty^2}$ was 4.37. Note that Γ_∞, the measured value of Γ for large r, is higher than for the other flows.

B. a significantly weaker jet, having about the same longitudinal momentum flux, and half-width, as the wake in the first, unmodified flow. Here velocity increment was 7.2%, and $\frac{|J|}{\rho\Gamma_\infty^2}$ was 0.37.

C. a jet whose momentum flux was just sufficient to eliminate the momentum deficit of the unmodified wake. Thus, after a certain period, it produced a field of approximately uniform axial mean velocity.

D. the above mentioned weak wake, with velocity decrement 7.2%, and $|J|/\rho\Gamma_\infty^2$ of 0.28.

E. a wake enhanced by a bluff body fixed to the central nacelle. Initially it was intended that this wake have a momentum decrement as large as the increment of the strong jet, and of the same physical extent. In practice it was impossible to create a wake of great enough momentum decrement without a very large halfwidth. In the end a machined hemispherical cup of diameter 38 mm, mounted with its convex surface downstream was used to give a wake of momentum flux decrement several times greater than the 'weak wake' though smaller than the strong jet. Maximum velocity decrement was 13.2% and $\frac{|J|}{\rho\Gamma_\infty^2} = 0.84$.

To check instrumentation two classical flows were also used, fully developed turbulent flow in a circular pipe and flow in an axisymmetric jet with still surroundings.

2.3 Hot Wire Anemometry

Measurements were made, in each of the flows, of the mean velocity field and Reynolds stress tensor, at a variety of positions at a given downstream station. A group of such points, either in a horizontal or vertical line, constituted a traverse. Traverses were generally performed at three downstream stations. To gather the desired information at each point, measurements of both mean and fluctuating signals were made, with a normal hot wire probe, and with a slanted hot wire probe with yaw angle $\alpha = 45°$ at each of six different azimuthal angles, ϕ (fig. 2). The values were $\phi = 0°, 45°, 90°, 135°, 180°, 270°$. The mean square values for 0° and 180° give predominantly $\overline{uv}$, for 90° and 270° $\overline{uw}$, and the 45° and 135° readings are used to extract $\overline{vw}$, but this procedure is indirect and less accurate.

2.31 Calibration

The output of the anemometer - lineariser combination was calibrated against a range of known air velocities. For convenience this was done in the wind tunnel, with the vortex generator at zero incidence and the probe away from the plane of the wake. Velocities were measured with total and static tubes, while tunnel speed was monitored by the pressure drop across the contraction. The extremely good repeatability and stability of calibration meant that careful least-squares determination of calibration constants were performed only periodically. At various times during a traverse the anemometer-lineariser mean output was checked against a standard velocity - that of the streaming flow without a vortex, i.e. with the wings at zero incidence, in a standard position away from the generator wake.

In addition inclined wires were calibrated in yaw and pitch to determine the longitudinal cooling constant k for use in the regular calibration, and in the analysis of data.

The stability of anemometer output was helped greatly by dust filtering down to about one micron and by the laboratory air conditioning. For small departures of probe cold resistance from standard, a compensating change in operating resistance was adequate (Guitton 1970)[15].

2.4 Positioning and Alignment of Probes

Increments in y and z coordinates of the probe were made with high accuracy. The orientation in azimuthal angle was well controlled.

Alignment of the probe in pitch and yaw is somewhat more difficult and affects measurements greatly. A first approximation to correct alignment was made by careful geometrical orientation. Alignment was further improved by checking the mean output of an inclined probe at a variety of azimuthal angles in the absence of a vortex. Once alignment was correct, the output in each would be the same for all tunnel positions in exactly parallel flow. In practice alignment was altered to minimize the errors at four cross stream locations. The final alignment is estimated to be accurate to within ±1/4° in pitch and yaw.

2.41 Centering the Probe in the Vortex

Traverses were made along tunnel

Text is missing.

Unprinted page
in the book.

Text is missing.
Unprinted Page
in the book.

B weak jet
C zero momentum increment flow
D weak wake
E strong wake

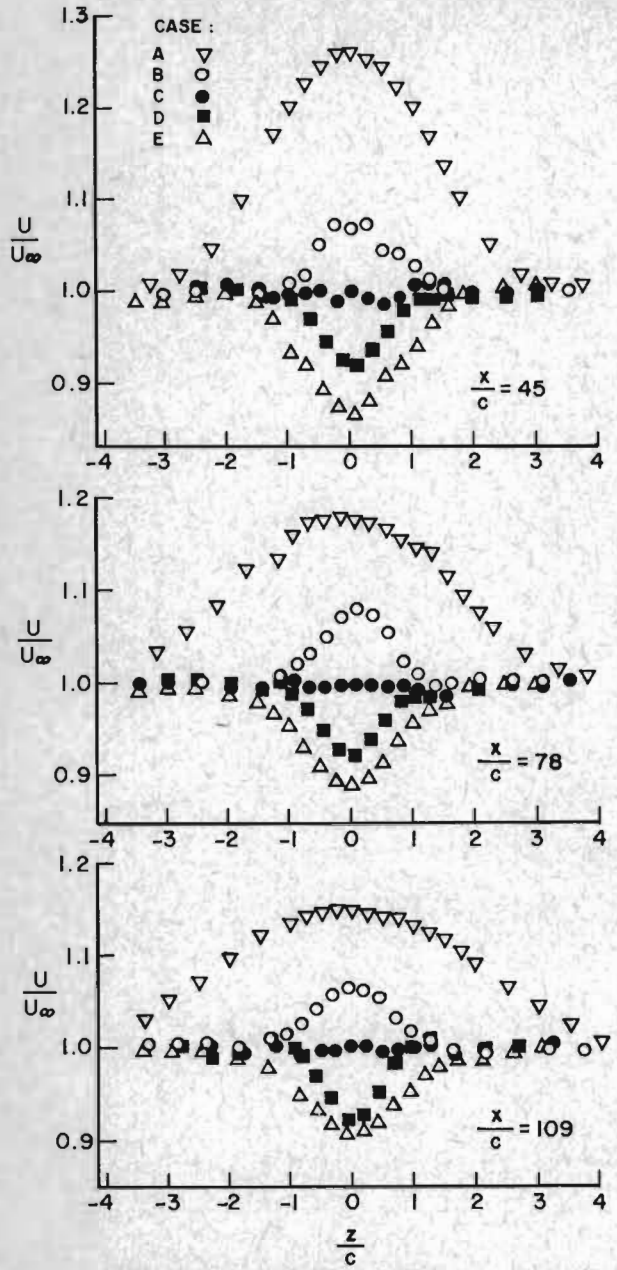

FIGURE 5 – LONGITUDINAL VELOCITY IN VORTEX

The profiles of mean longitudinal velocity are shown in fig. 5 and of the mean circumferential velocity in fig. 6.

It is immediately apparent that those flows with the greatest modification in longitudinal momentum flux $|J|$, whether caused by imposing a jet or wake on the vortex, experience a relatively rapid reduction in their tangential mean velocity profiles with downstream distance. For flows B, C, D, where the axial momentum increments and decrements are small or zero, the tangential velocity fields change very little.

3.11 Circumferential Velocity Field

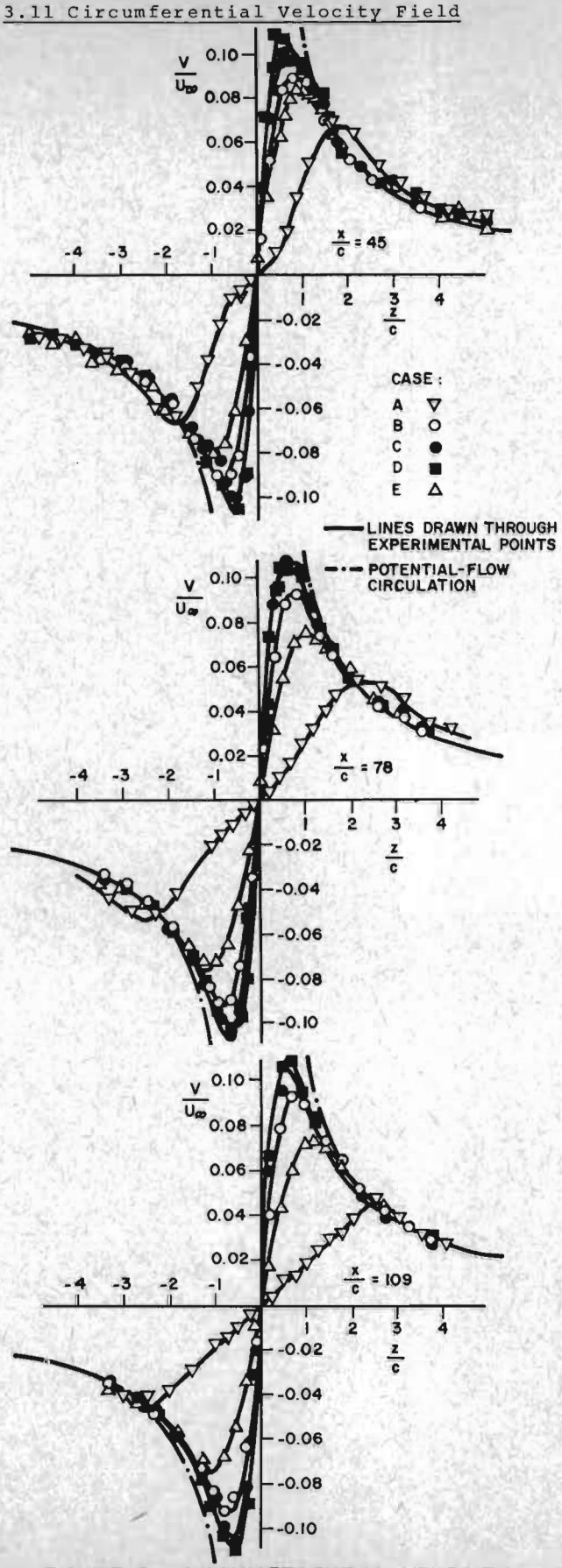

FIGURE 6 – CIRCUMFERENTIAL VELOCITY IN VORTEX

The mean flow fields have certain common features. All have a central core of close to solid body rotation, surrounded by an annulus of high strain rate. On each diagram the circulation of 0.75 m^2/sec predicted by potential-flow theory based on the vortex generator geometry is drawn. Lifting-line theory was used and a two-dimensional lift curve slope of 0.7 (2π) was assumed[13]. The experimental points for V at large r fall close to this line at all three stations, demonstrating that the flow in the outer annulus is potential. For x/c = 45, there is some indication of an increase in circulation at $r \approx 4r_1$. Such was predicted by Govindaraju and Saffman[22] and by Donaldson et al[23].

After a wrapping up region, about which little is known in detail, there is progressive diffusion of mean vorticity as the flow proceeds downstream. In order to check the development of axisymmetry of the flow some traverses were made along vertical diameters of the tunnel. The vertical traverses at the upstream station in the strong jet flow (A) and the weak wake (D) showed that at that station axial symmetry had been achieved very closely in each flow, (within ±2% of V_1) showing that wrapping up was almost complete. In addition, at the upstream station, in each flow, the vortex decay process appears to be under way, in view of the fact that the maximum circumferential velocities in flows A and E (with high $\frac{|J|}{\rho \Gamma_\infty z}$) are considerably lower than for the natural wake flow. Flow (D) has the highest maximum value of circumferential velocity at the first station, though at the second station it is exceeded by the zero momentum increment flow (C) for which $|J| = 0$. Flow (C) contains turbulence remaining from its generation which gives it a relatively high turbulence level and initial rate of diffusion. There are peculiarities in the circumferential velocity distribution in C and D at the upstream station, i.e. kinks in the distribution near the maximum value of V, although the flow is axisymmetric at this station.

The strong downstream diffusion of flows A and E, with their high $\frac{|J|}{\rho \Gamma_\infty z}$, make these flows very interesting as the basis of a method for modifying trailing vortices. The strong jet, (A) has two further features - firstly, the higher value of circulation at large radius, and secondly, the double structure of the core region. The first may be due to the increased flow over the wings of the vortex generator, induced by the jet, which causes an increased circulation. The two-structured vortex in the presence of the jet consists of an inner core of nearly solid body rotation surrounded by an annulus of greater angular velocity, which then merges into the highly sheared region where the point of maximum circumferential velocity is located. The innermost region is thought to be due to the high longitudinal velocities along the centreline. It should be noted that at successive downstream stations the region of solid body rotation expands into the neighbouring annulus of greater angular velocity without itself being speeded up.

3.2 Turbulence Measurements

A selection of the measurements are presented.

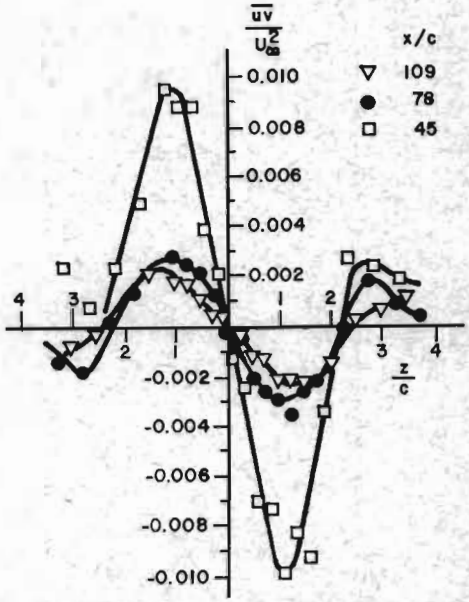

FIGURE 7 – $\overline{uv}$ FOR VORTEX WITH STRONG JET A

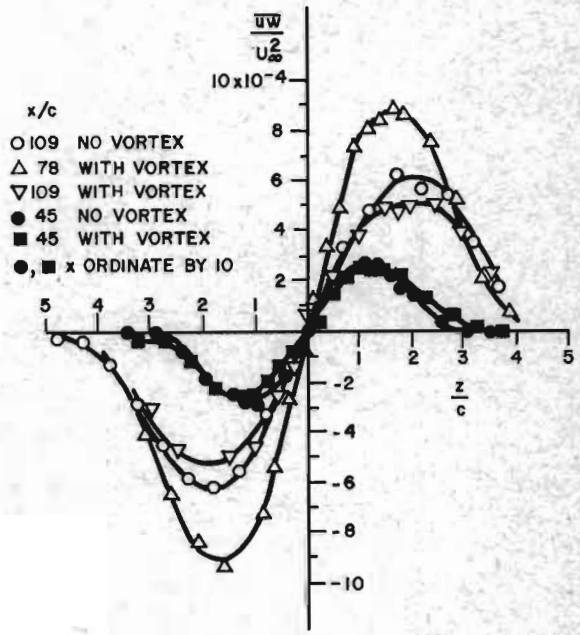

FIGURE 8 – $\overline{uw}$ WITH STRONG JET A

Figures 7,8, and 9 depict the Reynolds shear stress distributions for the strong jet. Comparison of $\overline{uw}$ for the strong jet with and without the vortex motion shows that the vortex has little effect on the shear stress distribution in the jet.

Figure 11 depicts three components of Reynolds stress at the middle station,

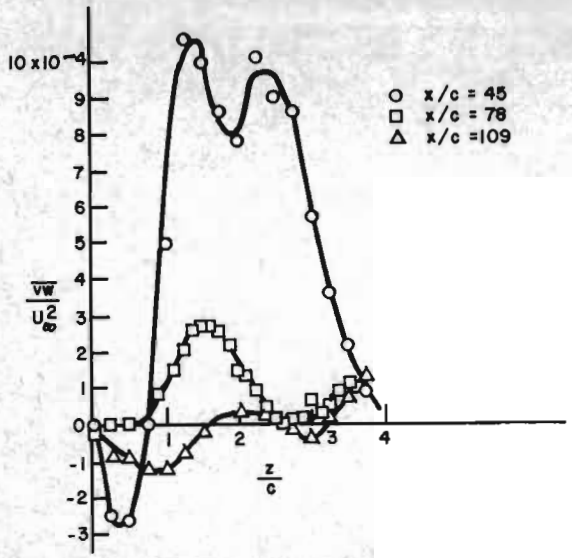

FIGURE 9 – $\overline{vw}$ FOR VORTEX WITH STRONG JET A

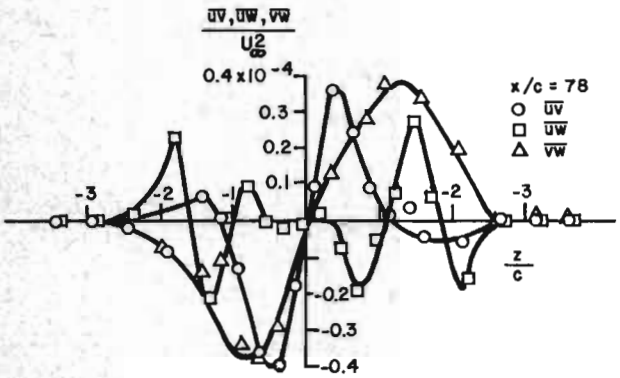

FIGURE 10 – $\overline{uv}, \overline{uw}, \overline{vw}$ FOR VORTEX D

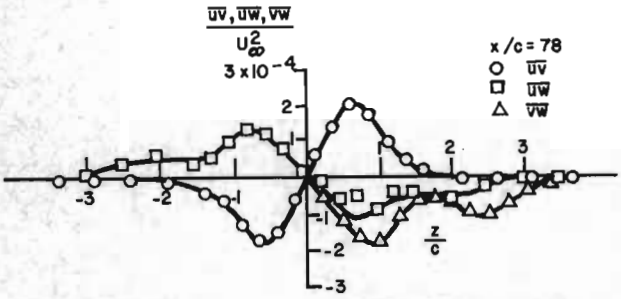

FIGURE 11 – uv, uw, vw FOR VORTEX WITH STRONG WAKE E

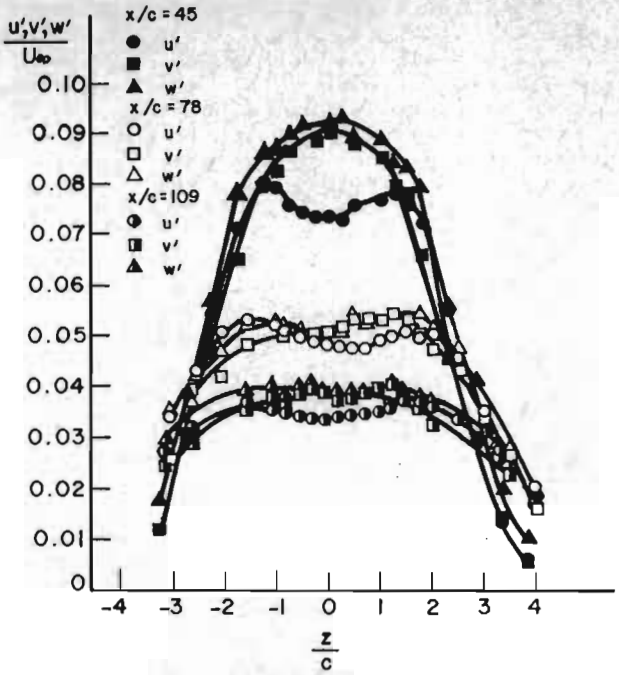

FIGURE 12 – TURBULENCE LEVELS IN THE VORTEX WITH STRONG JET A

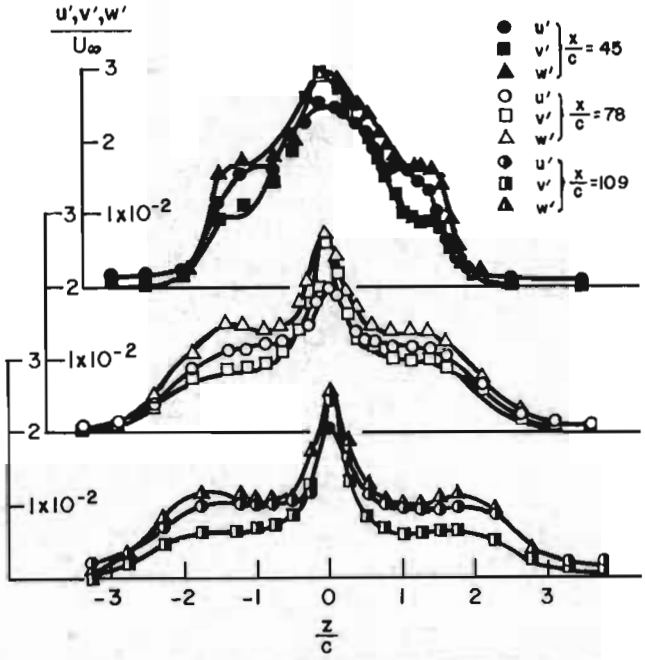

FIGURE 13 – TURBULENCE LEVELS u',v',w' FOR VORTEX D

for the vortex with strong wake, E.

These distributions illustrate clearly the great enhancement of all components of Reynolds stress by the longitudinal motion, when compared to an equivalent set of stress distributions for the vortex with wake D in figure 10.

The normal stress distributions in figures 12 and 13 show the remarkable increase in turbulence intensity for flows with large $|J|/\rho\Gamma^2$. This further leads to the idea that for a strong jet or wake the axial flow may dominate the vortex for at least part of its lifetime. In the weak wake flow, D, the narrow region of high turbulence is a consequence of the turbulent boundary layer on the central nacelle, and is confined by the vortex. The turbulence in this narrow region of relatively low shear stress suffers rapid decay.

In table 1 a group of physical quantities associated with turbulent vortices from laboratory and flight experiments are gathered together. The large variation in Squire's coefficient α from laboratory to

full scale can be seen. Two columns of eddy viscosity ratio $\frac{\nu_T}{\nu}$ are shown. The first is the eddy viscosity derived from the vortex motion and is determined by equating the observed value of the maximum circumferential velocity to Squire's value. The second is from the shear stress associated with the longitudinal flow, and is calculated directly from measurements of stress and strain rate. The remarkable similarity between the eddy viscosity in the vortex and jet indicates that the eddy viscosity might be treated as a scalar for flows A and E.

4. Analysis of the Flow

4.1 The Jet- or Wake-Dominant Vortex

Consider a vortex whose development is dictated by a scalar eddy viscosity set by a dominating jet or wake of axial momentum flux J, which is positive for a jet and negative for a wake. For convenience in calculating the development of the flow the jet or wake are assumed to have a small central axial velocity increment or decrement.

For a small increment round jet or wake in streaming flow, with a Gaussian longitudinal velocity profile, Newman[24]. (1967) gives

$$|\theta| = (1.2)\ L_0 \left(\frac{U_0}{U_\infty}\right)^{1/2} \qquad (1)$$

The shearing stress at $r=L_0$ is obtained from the growth and gives the eddy viscosity there, hence

$$\frac{L_0}{(x)^{1/3}\ |\theta|^{2/3}} = \left(\frac{2.88}{R_T}\right)^{1/3} \qquad (2)$$

where L_0 = the jet half width to the half velocity point
U_0 = maximum velocity increment
U_∞ = streaming flow velocity
θ, the momentum increment thickness is given by

$$\theta^2 = \left| \int_{-\infty}^{+\infty} \frac{U}{U_\infty}\left[\frac{U}{U_\infty} - 1\right] r\,dr \right|$$

x = downstream distance

$R_T = \frac{U_0 L_0}{\nu_T}$ eddy viscosity Reynolds number at $y = L_0$.

$|J|$ is related to θ by

$$\theta^2 = \frac{|J|}{\pi \rho U^2} \qquad (3)$$

Combining these four equations gives

$$\nu_T = C\ \frac{(|J|/\rho)^{2/3}}{x^{1/3}\ U_\infty^{1/3}} \qquad (5)$$

where $C = \frac{1}{R_T^{2/3}}\left[\frac{1}{\pi}\right]^{2/3}\frac{1}{1.44}\left[\frac{1}{2.88}\right]^{1/3}$

Note that eddy viscosity is dependent on x or time t, these two being related by $x=U_\infty t$.

For the vortex behaviour equation (6) from Newman (1959) describes the circumferential motion of a viscous vortex,

$$U_\infty \frac{\partial V}{\partial x} = \nu\left[\frac{\partial^2 V}{\partial r^2} + \frac{1}{r}\frac{\partial V}{\partial r} - \frac{V}{r^2}\right]. \qquad (6)$$

Substituting the value of eddy viscosity set by the jet, as given by (5),

$$U_\infty \frac{\partial V}{\partial x} = C\ \frac{(|J|/\rho)^{2/3}}{x^{1/3}\ U_\infty^{1/3}}\left[\frac{\partial^2 V}{\partial r^2} + \frac{1}{r}\frac{\partial V}{\partial r} - \frac{V}{r^2}\right]$$

that is,

$$U_\infty \frac{\partial V}{\partial x^{2/3}} = \frac{3}{2}\ C\ \frac{(|J|/\rho)^{2/3}}{U_\infty^{1/3}}\left[\frac{\partial^2 V}{\partial r^2} + \frac{1}{r}\frac{\partial V}{\partial r} - \frac{V}{r^2}\right] \qquad (7)$$

This is the equivalent of the transformation

$$x \to x^{2/3} \text{ and } \nu \to \frac{3}{2}\ C\ \frac{(|J|/\rho)^{2/3}}{U_\infty^{1/3}} \qquad (8)$$

Thus the solution gives a profile of circumferential velocity at r:

$$V = \frac{\Gamma_\infty}{2\pi r}\left(1 - \exp\left[-\frac{U_\infty^{4/3}\ r^2}{x^{2/3}\ 6C\,(|J|/\rho)^{2/3}}\right]\right) \qquad (9)$$

A quantity of great interest is V_1, the maximum circumferential velocity. It is this quantity that is a measure of the danger that a trailing vortex presents to other aircraft. From the solution given by Newman (1959) and employing the above transformation

$$V_1 = C'\ \Gamma_\infty\left[\frac{\rho U_\infty^2}{|J|\,x}\right]^{1/3} \qquad (10)$$

where $C' = \frac{0.639}{4\pi\,[(3/2)C]^{1/2}}$

It is interesting to note that the $x^{-1/3}$ decay agrees with Lilley's[25] empirical correlation of experimental results.

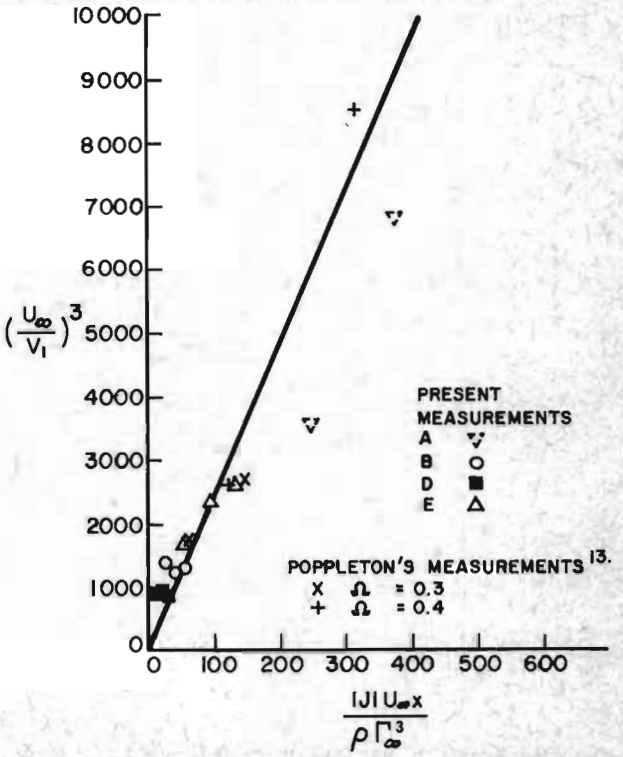

FIGURE 14 – COMPARISON WITH JET-DOMINANT THEORY

The experimental results are presented accordingly in Figure 14. The ordinate is $(U_\infty/V_1)^3$ and abscissa $\frac{|J|U_\infty x}{\rho\Gamma_\infty{}^3}$. A straight line, corresponding to equation (10), is drawn through the present data and through those of Poppleton's two jets, and gives a constant C' of 0.345. Data corresponding to the present strong jet is not used in determining C' because the circumferential velocity profile departs considerably from the exponential profile of equation (9), the results are however shown on figure 14. The value of C' is equivalent to an eddy viscosity Reynolds number, R_T of 62. R_T derived directly from the measured Reynolds stress and the strain rate is about 17.5 for the strong jet and 26 for the strong wake. In comparing the available data for small decrement round wakes, Rodi[26] has found that R_T can vary from about 25 for round wakes produced by slender bodies down to about 2 for very blunt bodies. It is expected that the presence of the vortex will reduce the level of turbulence in the jet or wake and thus cause R_T to lie at the high end of the range of experimental values.

4.11 The Range of Validity

The decrease of ν_T with increasing x suggests that the foregoing theory will no longer be valid far downstream. Presumably the jet-dominant theory ceases to apply when the maximum rate of strain in the longitudinal motion of the jet or wake becomes smaller than the maximum rate of strain in the rotational motion of the vortex.

The rotational velocity

$$V = \frac{\Gamma_\infty}{2\pi r}\left[1-e^{-k_1 r^2}\right]$$

where $k_1 = \dfrac{U_\infty^{4/3}}{6C\left[\dfrac{|J|x}{\rho}\right]^{2/3}}$

from (9) and the rate of strain is given by $-r\frac{\partial}{\partial r}(V/r)$. The maximum rate of strain occurs when $-\left\{e^{-k_1 r^2}\left[\frac{1}{k_1 r^2}+1\right]-\frac{1}{k_1 r^2}\right\}$ is a maximum i.e. when $k_1 r^2 = 1.79$ or $r = 1.19\, r_1$, where r_1 is the position of maximum rotational velocity.

Thus the maximum rate of strain in the rotational motion is

$$1.1\,\Gamma_\infty\left[\frac{\rho U_\infty{}^2}{|J|x}\right]^{2/3}$$

For the longitudinal motion the maximum value of $\left|\frac{\partial U}{\partial r}\right| = \left|.71\frac{U_0}{L_0}\right| = \frac{0.71R_T}{2(1.44)^2}\frac{U_\infty}{x} = 10.6\frac{U_\infty}{x}$

Hence the ratio of the two rates of strain, longitudinal/rotary,

$$\frac{\left[\left|\frac{\partial U}{\partial r}\right|\right]_{max}}{\left[-r\frac{\partial}{\partial r}\left(\frac{V}{r}\right)\right]_{max}} = S_r = 9.7\left(\frac{|J|}{\rho\Gamma_\infty{}^2}\right)^{2/3}\left(\frac{\Gamma_\infty}{U_\infty x}\right)^{1/3} \qquad (11)$$

Experimental ratios at the far downstream stations are:

Flow A:	5.0
Flow E:	1.6
Flow B:	0.9
Flow D:	0.75

4.2 The Two-Dimensional Vortex Far Downstream

Equation (11) indicates that the wake or jet does not remain dominant far downstream. Then previous theories, which ignore the presence of any variation of longitudinal velocity, become applicable. Squire's is an example of such a theory, independent of molecular viscosity and having a constant eddy viscosity. At large x, equation (6) holds, with constant eddy viscosity, ν_T.

It is necessary to find an appropriate value of $\nu_T/\Gamma_\infty(=\alpha)$ for the flow at large x. Typical values of α for laboratory flows are between 1×10^{-3} and 5×10^{-3}. For Rose and Dee's[26] flight experiments $\alpha = 0.2\times10^{-3}$. While this may not give the asymptotic value of α it is undoubtedly nearer than any other measured value.

A numerical computation of these vortex flows has recently been made by Phillips[16]. (1974) using the Launder, Reece and Rodi (1973)[30] model for second order closure of the Reynolds stress equations: their constants were used and the equations were restated in cylindrical polar coordinates. The calculations predict the early development of the vortex quite well and, in particular, indicate that deviation from the jet-dominant behaviour begins at a strain-rate ratio $S_r = 2$. Unfortunately the predictions of the far-field behaviour of cases B and D at the experimental Reynolds number are less convincing because the assumptions of local isotropy become suspect after $\frac{U_\infty x}{\Gamma_\infty} = 1000$. It is therefore not possible to choose the most appropriate value of α from these computations.

An approximate theory for the development of a vortex originally dominated by a jet or wake, which eventually becomes quasi-two-dimensional far downstream, is now obtained. It is postulated that the change-over from one type of vortex to the other occurs suddenly rather than gradually and that the strain rate ratio, S_r, which decreases in the downstream direction, has a value of unity at the point of change-over. This choice has also been influenced by the typical times for vortices to decay behind very large aircraft. It is also assumed that the far-field value of α is somewhere between 0.2×10^{-3} and 0.1×10^{-3}.

The solution for the two-dimensional vortex motion are those of Squire[6] and of Newman[7], and thus

$$V = \frac{\Gamma_\infty}{2\pi r}\left[1-e^{-k_2 r^2}\right] \quad \text{where} \quad k_2 = \frac{U_\infty}{4\nu_T X}.$$

X is measured from a hypothetical origin, which is not the same as the origin for x. The maximum velocity $V_1 = 0.1016\Gamma_\infty k_2^{1/2}$ and occurs at $k_2 r^2 = 1.256$.

At the change-over position, denoted by x_0 and X_0

$$1.0 = 9.7\left(\frac{J^2}{\Gamma_\infty^3 \rho^2 U_\infty x_0}\right)^{1/3}$$

Also $k_1 = k_2$ to match the rotational velocity profiles, so that

$$\frac{U_\infty}{4\alpha\Gamma_\infty X_0} = \frac{U_\infty^{4/3}}{6C\left[\frac{|J|\,x_0}{\rho}\right]^{2/3}}$$

Thus,

$$\left(\frac{U_\infty}{V_1}\right)^3 = \left(\frac{2}{0.1016}\right)^3 \alpha^{3/2}(X_0 - x_0 + x)^{3/2}\left(\frac{U_\infty}{\Gamma_\infty}\right)^{3/2} \quad (12)$$

Hence values of $\frac{U_\infty}{V_1}$ as a function of $\frac{U_\infty x}{\Gamma_\infty}$ can be computed for various values of the non-dimensional jet momentum $\frac{|J|}{\rho\Gamma_\infty^2}$. These are shown in Figure 15.

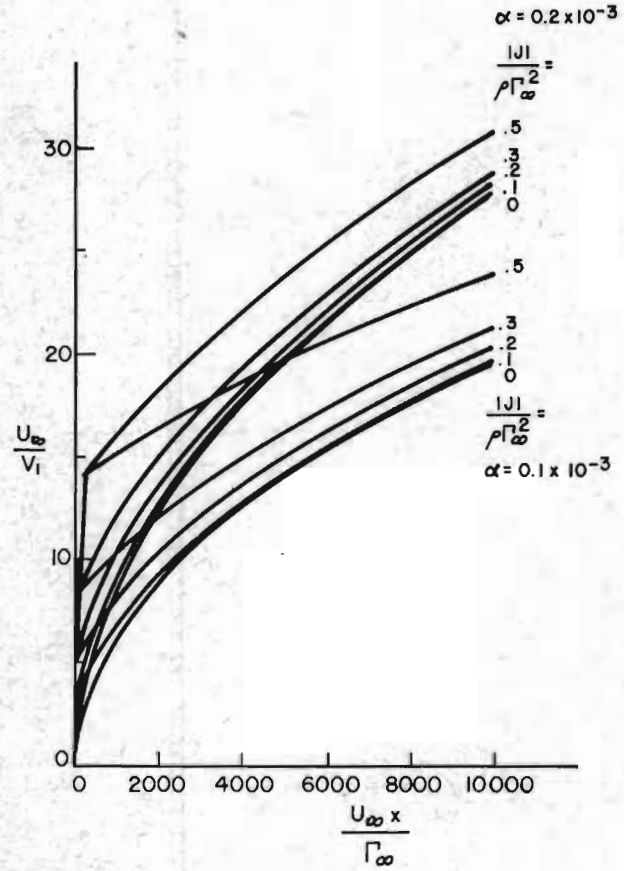

FIGURE 15 – HYBRID THEORY FOR MAXIMUM CIRCUMFERENTIAL VELOCITY IN VORTEX

It is seen the maximum velocity V_1 decays more slowly immediately after the change-over occurs ($\frac{U_\infty}{V_1}$ is smaller). In this figure the jet-dominant part of the flow is barely visible unless $\frac{|J|}{\rho\Gamma_\infty^2}$ exceeds about 0.2. Nevertheless the downstream values of $\frac{U_\infty}{V_1}$ are clearly affected by the presence of the jet or wake and this is due to the change of fictitious origin of the quasi-two-dimensional flow.

5. Discussion

The application of the theory to full scale will first be considered. It is clear that enhancing $|J|$ is a possible means of increasing the decay rate of a trailing vortex. This can be done either by blowing a jet which is strong enough to override the existing wake, or by increasing the momentum deficit of the wake by the introduction of some wake-producing body near the wing tip, as in the work of Corsiglia[28] et al.

For a Boeing 747 at take-off and landing speeds, that is at about 65 m/sec the curves of figure 15 can be used to estimate the effect of blowing a jet along the axis of each trailing vortex. The trailing vortex behind a wing tip without modification must first be considered. With a wing drag coefficient of .05, $\frac{|J|}{\rho\Gamma_\infty^2}$ is about 0.005 at take-off. Using an asymptotic value of $\alpha = 0.1\times10^{-3}$, after 10 minutes (a typical operational delay time[3]) $\frac{U}{V_1}$ is 11.6, so that V_1=17.25 ft/sec, which seems reasonable. If 10% of the total thrust of the four JT9D Pratt and Whitney engines is used for vortex modification $\frac{|J|}{\rho\Gamma_\infty^2}$ becomes 0.08 and the time for the maximum circumferential velocity to decay to a value of 17.25 ft/sec is reduced to 9.15 minutes. If 30% of the thrust is used, the time is 4.85 minutes. The improvement is increased if the acceptable values of U/V_1 are lowered.

A comparison of the combined theory with flight test results is difficult because $|J|$ is unknown. The wake of the wings, the bulk of which may be wrapped up in the vortex, can be estimated, but the proportion of the jet stream or propellor slipstream that enters the vortex cannot easily be estimated, and will act to reduce the apparent -J, though not necessarily the initial level of turbulence.

Comparisons have been made with the measurements of Rose and Dee using a Venom observation craft behind a Comet and by McCormick et al.[29] using a ground station behind a Piper Cherokee. In both cases $|J|$ was computed from an estimate of wing drag only. The results are shown in Fig. 16. The Cherokee results are probably unreliable because of the proximity of the ground and would only agree with the theory if the lower asymptotic value of α were chosen. The Comet measurements are in better agreement (the higher asymptotic value of α was based on these results) and they also exhibit the correct trend as $\frac{|J|}{\rho\Gamma_\infty^2}$

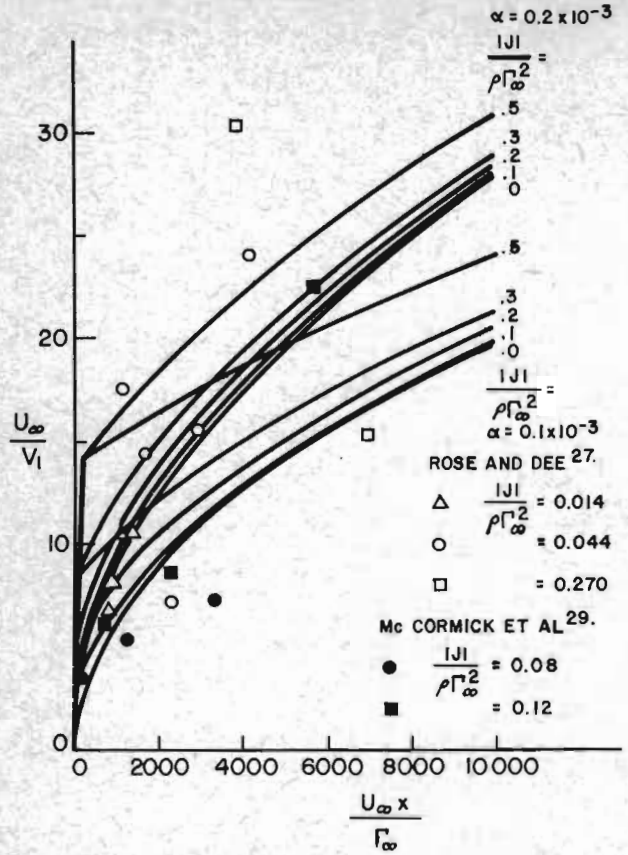

FIGURE 16 - COMPARISON WITH FULL-SCALE MEASUREMENTS

increases with flight speed. The results are not sufficiently accurate to indicate whether the limiting strain-rate ratio for the jet-dominant theory was chosen correctly at 1.0.

Finally the present theory provides a partial explanation for the apparent scale effect on the decay of trailing vortices. This variation with Reynolds number is unexpected since the flow is far from walls. The explanation is as follows. Vortices behind aircraft usually contain a wake-like axial motion due to the drag of the wing. This wake will be reduced if some fraction of the jet or propellor slipstream enters the vortex, particularly for aircraft with wing-mounted engines. Laboratory vortices, on the other hand, have a wake-like axial flow where the wake is produced mostly by the drag of the vortex generator. Referring to Fig. 15 $\frac{|J|}{\rho\Gamma_\infty^2} = \frac{2C_D}{C_L^2} A'$ where $A' = \frac{(2s')}{S}$, $2s'$ is the spacing of the rolled-up vortices and S is the wing area used in defining the drag and lift coefficients. Thus $\frac{|J|}{\rho\Gamma_\infty^2}$ is larger in the laboratory than in the full-scale situation at the same C_L, partly because of the above reasoning and partly because C_D increases with the reduction of Reynolds number. The abscissa $\frac{U_\infty x}{\Gamma_\infty} = A' \frac{x}{s'} C_L$, so that for a fixed number of vortex spans downstream $\frac{U_\infty x}{\Gamma_\infty}$ is the same for both laboratory and full scale. Thus $\frac{U}{V_1}$ is reduced with increasing scale in agreement with observation.

6. Conclusions

It has been shown experimentally that the introduction of a wake or jet in the centre of a single trailing vortex enhances the turbulence in the central region where the mean vorticity is otherwise constant and thereby significantly increases the rate of diffusion of mean vorticity. This appears to be a way of reducing the hazards associated with the persistence of trailing vortices from large, heavy, aircraft, although its usefulness depends on whether the associated thrust reduction or drag increase is acceptable.

An approximate theory has been developed for the effect by assuming that the jet with excess momentum flux J, or the wake with deficit of momentum flux -J, are sufficiently strong to impose their eddy viscosity on the vortex motion. The jet or wake are analysed by assuming that the velocities in them do not differ greatly from the streaming flow velocity U_∞. On this basis the maximum rotational velocity in the vortex V_1 is related to the circulation Γ_∞ and downstream distance x by the formula

$$V_1 = C'\Gamma_\infty \left(\frac{\rho U_\infty^2}{|J| x} \right)^{1/3}$$

C' has been obtained from the present experiments and equals 0.35. Thus the downstream distance, and hence the time, for V_1 to reach a prescribed level varies inversely as $|J|$.

This formula is valid as long as the maximum strain rate in the jet-wake is much greater than the maximum strain in the vortex. The requirement is that $\frac{J^2}{\Gamma_\infty^3 \rho^2 U_\infty x} > 10^{-3}$ approximately. Downstream a quasi two-dimensional theory is proposed.

It is suggested that in most practical situations vortices are affected by the presence of a wake at least in the initial phases of their development and that this may contribute to the apparent and unlikely Reynolds number dependence of vortices when they are treated as two-dimensional. It is observed that full-scale vortices decay less rapidly than small scale laboratory vortices when the scaling is assumed to be independent of viscosity. This may be due to the fact that the relative momentum deficit of the central wake gathered into the vortices is less in the full-scale situation for two reasons. Firstly, the drag coefficient of the wing and appendages is less at the higher Reynolds numbers, and secondly some momentum flux from the jet engines or propellers may be gathered into the vortices thereby reducing the momentum deficit $|J|$.

TABLE I

	Γ_0/ν	ν_T/ν	$\alpha\times10^3$	Λ	ν_T/ν
Present Data: (1=Upstream Station ℓ=45, 2=Middle Station ℓ=78, 3=Downstream Station ℓ=109)					
Flow A 1	5×10^4	1080	21.6	3.5	1450
2	"	1050	20.5	3.4	1140
3	"	846	16.9	3.1	900
Flow B 1	"	256	5.1	1.6	
2	"	116	2.3	1.1	
3	"	68.5	1.4	.87	
Flow C 1	"	166	3.3	1.35	
2	"	71.2	1.4	.9	
3	"	39	.8	.66	
Flow D 1	"	95	1.9	1.0	
2	"	71	1.4	.9	
3	"	39	.8	.66	
Flow E 1	"	316	6.3	1.87	334
2	"	220	4.4	1.56	261
3	"	150	3.1	1.32	152
Comparative Data, as given by Owen					
Rose & Dee	10^7	2000	0.2	1.22	
Dosanijh et al	2×10^3	10	5.0	.81	
Newman	2×10^4	30-50	2.0	.69-.89	
Templin	5×10^4	70	1.4	.84	
Mabey	5×10^4	77	1.7	1.01	

References

1. Crow, S.C. 1970 'Stability theory for a pair of trailing vortices', AIAA Journal, 8, No. 12, 2172.
2. Widnall, S.E. and Bliss, D.B., 1971 'Slender body analysis of the motion and stability of a vortex filament containing an axial flow', J. Fluid Mech., 50, part 2, 335.
3. Crow, S.C. 1971 Panel Discussion, Aircraft wake turbulence and its detection. Plenum Press (New York) Editors: J.H. Olsen, A. Goldburg, and M. Rogers.
4. Chevalier, H. 1973 'Flight test studies of the formation and dissipation of trailing vortices', Soc. Automotive Engineers Paper 730295.
5. Lamb, H. 1932 Hydrodynamics, Cambridge University Press, 6th ed., p. 592.
6. Squire, H.B. 1965 'The growth of a vortex in turbulent flow', Aeronautical Quarterly, XVI, 302, August 1965.
7. Newman, B.G. 1959 'Flow in a viscous trailing vortex', Aeronautical Quarterly, X, 149, May 1959.
8. Batchelor, G.K. 1964 'Axial flow in trailing line vortices', J. Fluid Mech., 20, 645.
9. Tam, K.K. 1973 'A note on the flow in a trailing vortex', Journal of Engineering Mathematics, 7, No. 1, 1.
10. Hoffman, E.R. and Joubert, P.N. 1963 'Turbulent line vortices', J. Fluid Mech., 16, part 3, 395.
11. Owen, P.R. 1970 'The decay of a turbulent trailing vortex', Aeronautical Quarterly, XXI, 69, February 1970.
12. Saffman, P.G. 1973 'Structure of turbulent line vortices', The Physics of Fluids, 16, No. 8, 1181.
13. Poppleton, E.D. 1971 'A preliminary experimental investigation of the structure of a turbulent trailing vortex', M.E.R.L. Rep. No. TN 71-1.
14. Vogel, W.M. 1968 Department of Mechanical Engineering, McGill University, Rep. TN68-1.
15. Guitton, D.E. 1968 'Correction of hot wire data for high intensity turbulence, longitudinal cooling, and probe interference', M.E.R.L. Rep. No. 68-6.
16. Phillips. W.R. 1974 M.Eng. Thesis, Department of Mechanical Engineering, McGill University, 1974.
17. Champagne, F.H. and Sleicher, C.A., 1967 'Turbulence measurements with inclined hot-wires. Part 2. Hot wire response equations', J. Fluid Mech. 28, Part 1, 177.
18. Laufer, J. 1954 'The structure of turbulence in a fully developed pipe flow', N.A.C.A. Report 1174.
19. Irwin, H.P.A.H. 1972 'The longitudinal cooling correction for wires inclined to the prongs and some turbulence measurements in fully developed pipe flow', M.E.R.L. Report No. TN 72-1.
20. Wygnanski, I. and Fiedler, H., 1969 'Some measurements in the self-preserving jet', J. Fluid Mech., 38, part 3, 577.
21. Smith, P.A. 1973 'Analog function unit design manual', M.E.R.L. Report TN 73-4.
22. Govindaraju, S.P. and Saffman, P.G. 1971 'Flow in a turbulent trailing vortex', The Physics of Fluids, 14, No. 10, 2074.

23. Donaldson, C du P., Sullivan, R.D. and Snedeker, R.S., 1971 'Theoretical and experimental study of the decay of isolated vortices', A.R.A.P. Tech. Memo 71-2, February, 1971.

24. Newman, B.G. 1967 'Turbulent jets and wakes in a pressure gradient', Fluid Mechanics of Internal Flow. Elsevier Publ. Co. - Amsterdam. Ed. Gino Sovran.

25. Lilley, G.M. 1964 'A note on the decay of aircraft trailing vortices', College of Aeronautics, Cranfield, Memo 22.

26. Rodi, W. 1972 'The prediction of free turbulent boundary layers by use of a two-equation model of turbulence', Ph.D. Thesis, Faculty of Engineering, Imperial College, London.

27. Rose, R. and Dee, F.W. 1963 'Aircraft vortex wakes and their effects on aircraft', R.A.E. Tech. Note No. 2934.

28. Corsiglia, V.R., Jacobson, R.A. and Chigier, N., 1971 'An experimental investigation of trailing vortices behind a wing with a vortex dissipator'. Aircraft wake turbulence and its detection, Plenum Press (New York). Eds: J.H. Olsen, A. Goldburg and M. Rogers, p. 229.

29. McCormick, B.W., Tangler, J.L. and Sherrieb, H.E., 1968 'Structure of trailing vortices', J. Aircraft 5, 260. May-June 1968.

30. Launder, B.E., Reece, G. and Rodi, W., 1973 'Development and application of a Reynolds stress turbulence closure', Imperial College, Mechanical Engineering Department, HTS/73/31.

AIRCRAFT TRAILING VORTEX INSTABILITIES

William P. Jones and Howard L. Chevalier
Texas A&M University, College Station, Texas

Abstract

A brief summary is given of the results of flight test studies of trailing vortices carried out at Texas A&M University. The instability of a pair of trailing vortices due to mutual interaction is fully discussed and theoretical predictions of the wavelength of the vortex oscillations that develop in the far wake of an airplane are compared with values determined from photographic records of the wake behavior of a DeHavilland Beaver DHC-2 aircraft. The different types of instability that can develop with single vortices are also considered, including the vortex bursting phenomenon that occurs with vortices that separate from the leading edges of highly swept wings at incidence. A technique for inducing earlier breakdown and dissipation of the vortices than would occur normally is described.

I. Introduction

Concurrently with the development of the Boeing 747 and other large airplanes, much effort has been devoted to research on aircraft wake turbulence, particularly for low altitude flight. This was because the regions of high velocity generated by the trailing vortices of such heavy aircraft are a source of potential danger to other aircraft that might penetrate them. On a calm day, the vortex wake of a heavy transport plane that had just landed or taken off would persist over the runway for several minutes and make it dangerous for any other aircraft to land. In fact several accidents to light aircraft have occurred due to the pilot flying inadvertently into the wake of a much heavier aircraft. To avoid such hazards, traffic controllers at airports must have some idea of the length of time it takes for the vortex wake of a large aircraft to dissipate and to become relatively harmless to other aircraft. Hence, from the point of view of safer flying, it is important to know as much as possible about the behavior of vortex wakes, their structure and the time they take to dissipate.

In 1970, an important symposium on the subject of Aircraft Wake Turbulence[1] was held in Seattle to draw attention to the need for more research to determine the characteristics and behavior of trailing vortices and to assess the potential danger they would present to aircraft at busy airports. The meeting, sponsored by Boeing Scientific Research Laboratories and the U.S. Air Force Office of Scientific Research, resulted in a number of valuable reports which have been published in the proceedings of that symposium. These collected papers provide a useful background of information on trailing vortices and give a fairly complete survey of the state of knowledge at that time as well as indicating where further work is required. More particularly, they show that there is a need for more data on trailing vortices obtained in actual flight. Some of the reports describe in very general terms the results of observations made of the characteristics of trailing vortices as revealed by smoke trails from smoke bombs mounted on towers alongside the runway. When there is a cross wind, the wake drifts across the tower and the presence of the trailing vortex is clearly shown by the vortical pattern formed. An alternative scheme is to build a large tufted screen and to let the vortex again drift across it. Both schemes, however, have the disadvantage that the presence of the tower in the one case and the supporting structure of the screen in the other can influence the trailing vortex and possibly cause it to change its form. For this reason, it is desirable to use techniques of observation in which the trailing vortices are not obstructed in any way. A flow visualization scheme in which the vortex cores are seeded by smoke issuing from smoke bombs suitably mounted on the wings of the vortex generating aircraft has proved to be very satisfactory. This method has been used extensively at the Flight Mechanics Laboratory at Texas A&M University and detailed observations have been made of vortex wakes for a range of flight conditions in calm and gusty weather.[2] Attention was mainly devoted to the study of trailing vortex instabilities. The results obtained are briefly summarized in this paper and, as will be shown, confirm some theoretical deductions regarding the unstable characteristics of aircraft trailing vortices.

II. Instability Of A Pair Of Vortices

The stability of a pair of trailing vortices was first considered by S. C. Crow[3] who was able to show that the vortices would become unstable under certain conditions. In his analysis, he assumed that the vortices were given a small wave-like disturbance and then investigated the effects of mutual interaction and self-induction on the ensuing motion. The velocity induced at a point of one vortex can be expressed in terms of integrals taken along the lengths of the vortices. The integral corresponding to the self-induced velocity of a vortex at a point on itself is, however, divergent and to obtain a finite answer, Crow had to use the 'cut-off integral' method which introduces an empirical factor in his analysis. This involved cutting off a length d of the vortex on each side of the point on it at which the self-induced velocity was to be calculated. The choice of a suitable value for d was made by applying the 'cut-off integral' technique to problems whose exact solutions are known, e.g., that of calculating the translational speed of a vortex ring. In this way, it was determined that a value $d = 0.321\ c$ would give the correct answer, c being the core diameter of the vortex. According to Spreiter and Sacks,[4] the trailing vortices behind an elliptic wing of total span s would be separated by a distance, $b = \frac{\pi}{4} s$, and each vortex would have a core diameter, $c = 0.197b$. Having

chosen the appropriate value for d, Crow was then able to reduce the problem to an eigenvalue problem and to determine the stability characteristics of the trailing vortices. His analysis revealed that the most likely mode of instability of a pair of parallel line vortices would be in the form of symmetrical sinusoidal oscillations of the vortices in planes inclined at angles of $\pm$ 48° to the horizontal as sketched in Figure 1.

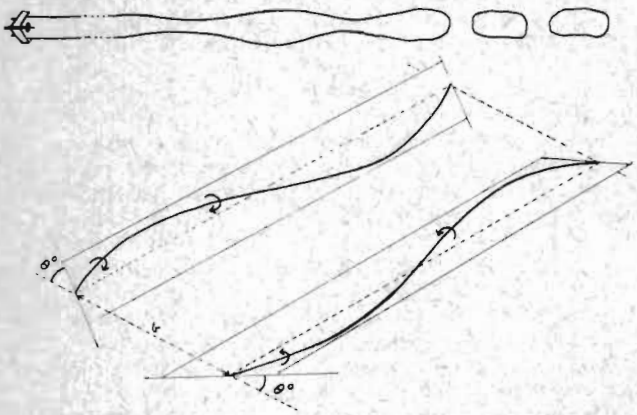

FIGURE 1. INSTABILITY OF A PAIR OF VORTICES

The wavelength of the oscillations was estimated to be 8.6 b (or 6.8s) and their rate of growth was found to be relatively slow. According to Ref. 3, the amplitude of the oscillation would increase by a factor e in time, $t = A_R b/C_L V_o$. For a B-47 airplane, travelling at V_o = 720 f.p.s., Crow gives a value of 21 secs. for t which implies that in 60 secs. the amplitude of the vortex oscillations would be magnified 17.4 times. When the oscillations become sufficiently large, the vortices touch and combine to form a series of closed loops which eventually disperse. Although the structure and axial velocity distributions within the vortex cores are not taken into account in Crow's analysis, his general conclusions have been amply confirmed by flight data.

In a recent paper, H. Chevalier[2] describes the results of a series of flight tests made to study the formation and dissipation of trailing vortices. The two aircraft used were a DeHavilland Beaver DHC-2 and a Beechcraft T-34B. Smoke bombs were attached below the wings of each aircraft near the tips and, when activated by the pilot, they seeded the cores of the trailing vortices with smoke as illustrated in Figure 2. The smoke trails produced were then photographed from above by a chase airplane at altitude and from the ground. Figure 3 is a photograph of the pair of trailing vortices generated by the DeHavilland Beaver taken from a following plane. The Crow type instability of the wake is clearly demonstrated. No measurements were made of the inclination of the planes of oscillation of the trailing vortices but they were observed to be about $\pm$ 45° to the horizontal and to be roughly in accord with Crow's prediction. Measurements of the wavelengths of the unstable motion of the wakes of the Beaver and T-34B aircraft were obtained from pictures of their trailing vortices taken from the ground.

(A) DEHAVILLAND BEAVER DHC-2

(B) BEECHCRAFT T-34B

FIGURE 2. SMOKE SEEDING OF VORTEX CORES

The wakes were photographed through a 6 ft. x 6 ft. wire grid mounted 10 ft. above the camera at ground level as shown in Figure 4. A clock mounted in its field of view and the frame speed of the movie camera were used to measure the time elapsed. The wire grid provided a reference coordinate system for measuring distances parallel to the ground and altitude. Values of height above the ground deduced from photographs of the airplane and its wake were checked against the airplane's altitude meter readings and the airplane's wing span was used to check measurements of distances.

Moving and still pictures of the trailing vortex wake were taken for straight and level flights at speeds of about 70, 80, 90, and 110 knots at an altitude of about 1000 ft. Most of the tests were made in the early morning when there was little atmospheric turbulence to influence wake stability and dissipation. For comparison purposes, however, some tests were carried out under various degrees of atmospheric turbulence and in slight cross winds of 3-10 knots. While the data obtained